Copper(II) Coordination Polymers and Complexes Derived from Aminoalcohols and Aromatic Carboxylic Acids: Synthesis, Structural Characteristics and Applications

Sara S. P. Dias[1], Vânia André[1], Marina V. Kirillova[1], Julia Kłak[2], Alexander M. Kirillov[1]

[1]Centro de Química Estrutural, Complexo I, Instituto Superior Técnico, Universidade de Lisboa, Av. Rovisco Pais, 1049-001, Lisbon, Portugal. E-mail: kirillov@ist.utl.pt

[2]Faculty of Chemistry, University of Wrocław, ul. F. Joliot-Curie 14, 50-383 Wroclaw, Poland

Abstract

This work describes the self-assembly synthesis, characterization and applications of eight new compounds, namely $[Cu_2(\mu\text{-dmea})_2(\mu\text{-nda})(H_2O)_2]_n\cdot 2nH_2O$ (**1**), $[Cu_2(\mu\text{-Hmdea})_2(\mu\text{-nda})]_n\cdot 2nH_2O$ (**2**), $[Cu_2(\mu\text{-Hbdea})_2(\mu\text{-nda})]_n\cdot 2nH_2O$ (**3**), $[Cu_2(H_4etda)_2(\mu\text{-nda})]\cdot nda\cdot 4H_2O$ (**4**), $[Cu_3(\mu_2\text{-}H_3bis\text{-}tris)_2(\mu_2\text{-Hhpa})_2]\cdot H_2O$ (**5**), $[Cu_3(\mu_2\text{-}H_2tea)_2(\mu_2\text{-hpa})(\mu_3\text{-hpa})]_n$ (**6**), $[Cu_4(\mu_4\text{-}H_2etda)(\mu_5\text{-}H_2etda)(sal)_2]_n\cdot 10H_2O$ (**7**) and $[Cu_4(\mu_4\text{-Hetda})_2(Hpmal)_2(H_2O)]\cdot 7.5H_2O$ (**8**) derived from various aminoalcohols [*N*,*N*′-dimethylethanolamine (Hdmea), *N*-methyldiethanolamine (H_2mdea), *N*-butyldiethanolamine (H_2bdea), *N*,*N*,*N*′,*N*′-tetrakis(2-hydroxyethyl)ethylenediamine (H_4etda), bis(2-hydroxyethyl)amino-tris(hydroxymethyl)methane (H_5bis-tris) or triethanolamine (H_3tea)] and 2,6-naphthalenedicarboxylic (H_2nda), homophthalic (H_2hpa), salycilic (H_2sal) or phenylmalonic (H_2pmal) acids. The obtained products were characterised by IR, ESI−MS(±), thermogravimetric, elemental and single crystal X-ray diffraction analysis. Structural elucidation of the compounds gave rise to the following conclusions: **1**–**3** are 1D coordination polymers assembled from dicopper(II) aminoalcohol blocks and μ-nda linkers, **4** is a discrete 0D dimer composed of two $[Cu(H_4etda)]^{2+}$ fragments interlinked by the μ-nda moiety, **5** is a discrete 0D trimer with symmetric $[Cu_3(\mu\text{-O})_4(\mu\text{-COO})_2]$ core, **6** is a zigzag 1D coordination polymer with asymmetric $[Cu_3(\mu\text{-O})_3(\mu\text{-COO})_2]$ core, **7** is a 1D coordination polymer with single-open cubane $[Cu_4(\mu_2\text{-O})(\mu_3\text{-O})_3]$ core and **8** is a 0D tetramer with double-open cubane $[Cu_4(\mu_2\text{-O})_2(\mu_3\text{-O})_2]$ core. An intense pattern of intermolecular (O–H···O) hydrogen bonds provides the extension of the structures into distinct supramolecular networks [1D → 3D (**1**, **2**, **7**), 1D → 2D (**3**, **6**) and 0D →3D (**4**, **5**, **8**)]. Their topological analysis was performed, disclosing some rare (**1**, **3**, **5** and **6**) or even undocumented (**2**, **4**, **7** and **8**) topological types. The magnetic susceptibility studies of **1**–**3** indicate a strong antiferromagnetic coupling between the Cu(II) atoms through the μ-alkoxo bridges [J = −470(2), −100(2) and −590(1) cm^{-1}, respectively] and a predominant ferromagnetic coupling [J = 39.1(1) and 29.5(1) cm^{-1}, respectively] within the mixed-bridged tricopper(II) cores in **5** and **6**. In contrast, **4** is devoid of any significant magnetic interaction within the dicopper(II) units. Finally, compounds **5**–**8** were also applied as rather efficient bio-inspired pre-catalysts for the mild homogeneous oxidation, by aqueous H_2O_2 at 50°C in acidic MeCN/H_2O medium, of cyclohexane to cyclohexanol and cyclohexanone with overall yields up to 27% based on the alkane.

Keywords: coordination polymers, copper(II) complexes, crystal structures, catalysis, magnetism.

Introduction

Within the vast development of crystal engineering research in recent years, the design of novel molecular materials bearing diverse multicopper(II) cores with promising functional properties has attracted an increased attention in view of the versatile redox, magnetic, biological, catalytic and coordination behavior of copper ions.[1] In many cases, rather unusual multicopper(II) aggregates of diverse nuclearity can be constructed via simple self-assembly protocols employing a variety of organic building blocks.[2,3] Aiming at searching for such organic molecules, we have focused our attention on some aminoalcohols as main building blocks, namely, H_5bis-tris, H_3tea, H_2mdea, H_2bdea, Hdmae and H_4etda; some of them are commonly applied as buffers in biochemistry and molecular biology (Figure 1).[4] As potential linkers, we have chosen aromatic carboxylic acids, namely H_2nda, H_2sal, H_2pmal and H_2hpa (Figure 2). In spite of their commercial availability, aqueous solubility and coordination versatility, the application of some of these aminoalcohols and carboxylic acids as potentially multidentate building blocks in crystal engineering of mixed-ligand multicopper materials has remained underexplored.[5]

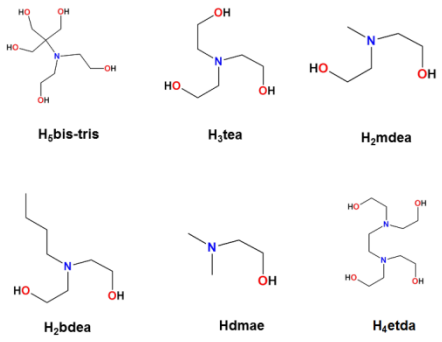

Figure 1. Structural formulae of aminoalcohol building blocks.

However, some notable examples of polynuclear Cu(II) compounds derived from H_3tea, Hdmae and carboxylic acids have been documented[6–8]. We report herein the aqueous medium self-assembly synthesis (Scheme 1) of compounds **1**–**8** that comprise di-, tri- or tetracopper(II) aminoalcohol cores (Scheme 2), their spectral characteristics, crystal structures, thermogravimetric, magnetic and catalytic properties.

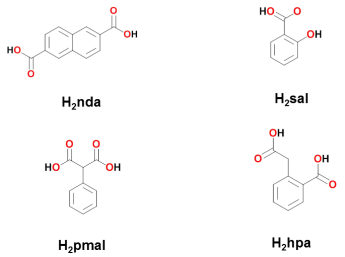

Figure 2. Structural formulae of aromatic carboxylic acids as building blocks.

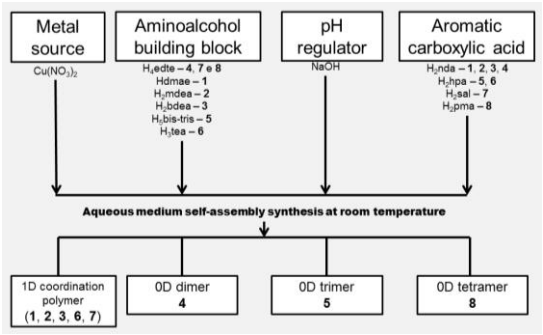

Scheme 1. Synthesis of **1**–**8** by aqueous medium self-assembly.

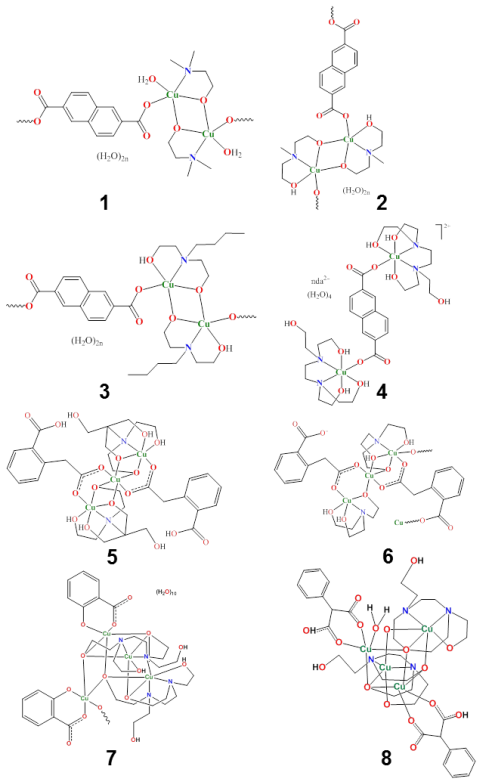

Scheme 2. Structural formulae of **1**–**8**.

Experimental section

Materials and Methods

All synthetic work was performed in air and at room temperature (~25°C). C, H and N elemental analyses were carried out by the Microanalytical Service of the IST. Infrared spectra (4000–400 cm^{-1}) were recorded on a JASCO FT/IR-4100 instrument in KBr pellets. ESI−MS(±) spectra were run on a 500-MS LC Ion Trap instrument (Varian Inc, Alto Palo, CA, USA) equipped with an electrospray (ESI) ion source. The thermogravimetric analyses (TGA) were carried out on a Setaram Setsys TG–DTA 16 instrument by heating the crystalline samples (8–12 mg) of **1**–**6** under N_2 at the 10 °C/min rate in the 30−750 °C temperature range. The crystal structures data were collected on a Bruker AXS-KAPPA APEX II diffractometer with graphite-monochromated radiation (Mo Kα, λ=0.17073 Å) at 273-303 K (**1**–**4**, **8**) or 150 K (**5**–**7**). The magnetization of the powdered samples **1**–**6** were measured over the 1.8–300 K temperature range using a Quantum Design SQUID–based MPMSXL–5-type magnetometer.

Synthesis and Characterisation of 1–8

To 10 mL of an aqueous 0.1 M solution of $Cu(NO_3)_2{\cdot}3H_2O$ (1 mmol) was added 1 mmol of an aqueous 1 M solution of aminoalcohol (Hdmea for **1**, H_2mdea for **2**, H_2bdea for **3**, H_5bis-tris for **5** and H_3tea for **6**) and 0.5 mmol of H_4etda for **4**, **7** and **8** with continuous stirring at r.t. Then, an organic linker, 0.5 mmol of (H_2nda for **1**–**4** and H_2pmal for **8**) and 1 mmol of (H_2hpa for **5**, **6** or H_2sal for **7**), and finally an aqueous 1 M solution of NaOH (3 mmol; up to pH ~8) for **1**–**8** was added to the reaction mixture. The resulting solution was stirred for 1 day and then filtered off. The filtrate was left to evaporate in a beaker at r.t. Grayish blue (**1**), blue (**2**, **4**, **6**), cyan-blue (**3**, **5**) and green (**7**, **8**) crystals (including those of X-ray quality) were formed in 1–3 weeks, then collected and dried in air to furnish the compounds **1**–**8** in ~50% yield, based on copper(II) nitrate.

$[Cu_2(\mu\text{-dmea})_2(\mu\text{-nda})(H_2O)_2]_n{\cdot}2nH_2O$ (**1**). Anal. calcd for **1**+0.5H_2O: $Cu_2C_{20}H_{34}N_2O_{10}{\cdot}0.5H_2O$ (MW 598.6): C 40.13, H 5.89, N 4.68; found: C 40.02, H 5.61, N 4.48. Compound **1** is barely soluble in MeCN, Me_2CO and DMSO. IR (KBr, cm^{-1}): 3379 (vs) ν(H_2O), 3003 (w) and 2967 (w) ν_{as}(CH), 2886 (w) and 2858 (w) ν_s(CH), 1617 (vs) and 1585 (s) ν_{as}(COO), 1392 (vs) and 1362 (vs) ν_s(COO), 1497 (w), 1469 (w), 1326 (w), 1275 (w), 1247 (w), 1187 (m) and 1140 (w) ν(C−X) (X = C, N), 1085 (s) and 1071 (s) ν(C–O), 1023 (w), 1016 (w), 978 (w), 948 (m), 904 (m), 847 (w), 799 (s), 789 (s), 661 (w), 644 (w), 589 (w), 526 (w), 488 (w), 476 (w), 427 (w), 418 (w). ESI−MS(±) (MeCN), selected fragments with relative abundance >20%. MS(+): *m/z*: 373 (30%) $[Cu_2(dmea)_2(H_2O)_2 + 2H_2O + H]^+$, 330 (100%) $[Cu(dmea)_2 + 5H_2O + H]^+$, 282 (60%) $[Cu(dmea)_2 + CH_3CN + H]^+$ 152 (20%) $[Cu(Hdmea)]^+$; MS(–): *m/z*: 295 (30%) $[Cu(H_2O)(nda) – H]^-$, 251 (100%) $[Hnda + 2H_2O]^-$.

$[Cu_2(\mu\text{-Hmdea})_2(\mu\text{-nda})]_n{\cdot}2nH_2O$ (**2**). Anal. calcd for **2**: $Cu_2C_{22}H_{34}N_2O_{10}$ (MW 613.6): C 43.06, H 5.59, N 4.57; found: C 43.51, H 5.67, N 4.50. Compound **2** is barely soluble in MeOH and EtOH. IR (KBr, cm^{-1}): 3510 (m), 3408 (s br.) and 3189 (s br.) ν(H_2O/OH), 2973 (w) ν_{as}(CH), 2861 (m) ν_s(CH), 1615 (s) and 1582 (s) ν_{as}(COO), 1386 (s) and 1361 (vs) ν_s(COO), 1496 (w), 1460 (w), 1190 (m) ν(C−X) (X = C, N), 1088 (s) ν(C–O), 1656 (w), 1139 (w), 1031 (w), 993 (m), 939 (w), 902 (m), 793 (s), 646 (m), 598 (w), 522 (w), 479 (m). ESI−MS(±) (MeOH), selected fragments with relative abundance >20%, MS(+): *m/z*: 361 (20%) $[Cu_2(Hmdea)_2 + H]^+$, 274 (25%) $[Cu(mdea)_2 + MeO]^+$, 120 (40%) $[H_2mdea + H]^+$; MS(–): *m/z*: 215 (100%) $[Hnda]^-$.

[Cu_2(μ-Hbdea)$_2$(μ-nda)]$_n$·2$n$$H_2O$ (**3**). Anal. calcd for **3**: $Cu_2C_{28}H_{46}N_2O_{10}$ (MW 697.8): C 48.20, H 6.64, N 4.01; found: C 48.34, H 6.60, N 3.97. Compound **3** is barely soluble in MeOH and MeCN. IR (KBr, cm^{-1}): 3449 (s br), 3370 (sh.) and 3188 (m br.) ν(H_2O/OH), 2953 (m) and 2922 (w) ν_{as}(CH), 2848 (m) ν_s(CH), 1609 (s) and 1582 (s) ν_{as}(COO), 1385 (vs) and 1352 (s) ν_s(COO), 1490 (w), 1462 (w), 1191 (w) ν(C−X) (X = C, N), 1088 (m) ν(C–O), 1035 (w), 979 (w), 900 (w), 783 (m), 662 (w), 582 (w), 559 (w), 481 (w). ESI−MS(±) (MeOH), selected fragments with relative abundance >20%. MS(+): *m/z*: 445 (10%) $[Cu_2(Hbdea)_2 + H]^+$, 384 (10%) $[Cu(Hbdea)_2 + H]^+$, 162 (100%) $[H_2bdea + H]^+$; MS(–): *m/z*: 215 (100%) $[Hnda]^-$.

[Cu_2(H_4etda)$_2$(μ-nda)]·nda·4H_2O (**4**). Anal. calcd for **4**: $Cu_2C_{44}H_{68}N_4O_{20}$ (MW 1100.1): C 48.04, H 6.23, N 5.09; found: C 48.34, H 6.23, N 5.06. Compound **4** is barely soluble in MeCN, Me_2CO and DMSO. IR (KBr, cm^{-1}): 3457 (vs br.) ν(H_2O/OH), 2975 (w) ν_{as}(CH), 2902 (w) ν_s(CH), 1605 (s) and 1574 (s) ν_{as}(COO), 1395 (vs) and 1356 (s) ν_s(COO), 1494 (w), 1456 (w), 1195 (m) and 1262 (w) ν(C−X) (X = C, N), 1061 (s) ν(C–O), 1148 (w), 926 (w), 875 (w), 797 (m), 763 (w), 737 (w), 646 (w), 487 (w). ESI−MS(±) (MeCN), selected fragments with relative abundance >20%. MS(+): *m/z*: 362 (10%) $[Cu_2(Hetda)]^+$, 278 (100%) $[Cu(nda) + H]^+$, 237 (35%) $[H_4etda + H]^+$; MS(–): *m/z*: 251 (100%) $[Hnda + 2H_2O]^-$.

[Cu_3(μ_2-H_3bis-tris)$_2$(μ_2-Hhpa)$_2$]·H_2O (**5**). Anal. calcd for **5**: $Cu_3C_{34}H_{50}N_2O_{19}$ (MW 981.4): C 41.61, H 5.14, N 2.85; found: C 40.98, H 5.34, N 2.71. IR (KBr): 3445 (m br) and 3176 (w br) ν(H_2O/OH), 2985 (w) ν_{as}(CH), 2929 (w) ν_s(CH), 1603 (m sh) and 1562 (vs) ν_{as}(COO), 1418 (m sh) and 1388 (s br) ν_s(COO), 1486 (m), 1236 (w), 1187 (w), 1140 (w), 1089 (w), 1049 (w), 1038 (s) 1006 (w), 931 (w), 906 (w), 860 (w), 816 (w), 770 (w), 736 (m), 675 (m), 636 (w), 587 (w), 553 (w), 497 (w), 468 (w), 437 (w), 423 (w).

[Cu_3(μ_2-H_2tea)$_2$(μ_2-hpa)(μ_3-hpa)]$_n$ (**6**). Anal. calcd for **6**: $Cu_3C_{30}H_{40}N_2O_{14}$ (MM 843.3): C 42.73, H 4.78, N 3.32; found: C 42.58, H 4.80, N 3.31. IR (KBr): 3330 (m br) ν(OH), 3013 (w) and 2975 (w) ν_{as}(CH), 2915 (w), 2871 (w) and 2838 (w) ν_s(CH), 1605 (s sh) and 1569 (vs) ν_{as}(COO), 1414 (s sh) and 1396 (vs) ν_s(COO), 1485 (w), 1466 (w), 1455 (w), 1312 (w), 1270 (m), 1228 (w), 1153 (w), 1140 (w), 1085 (s), 1067 (m), 1022 (w), 1006 (w), 963 (w), 932 (w), 894 (m), 859 (w), 809 (w), 768 (w), 742 (m), 730 (m sh), 703 (w), 670 (w), 647 (w), 603 (w), 574 (w), 554 (w), 516 (w), 451 (w), 420 (w), 407 (w).

[Cu_4(μ_4-H_2etda)(μ_5-H_2etda)(sal)$_2$]$_n$·10H_2O (**7**). Anal. calcd for **7**-3H_2O: $Cu_4C_{34}H_{66}N_4O_{21}$ (MW 1121.1): C 36.42, H 5.93, N 5.00; found: C 36.11, H 5.67, N 4.87. Compound **7** is slightly soluble in H_2O, MeOH, EtOH and MeCN. IR (KBr): 3362 (s br) ν(OH), 2864 (m) ν_s(CH), 1602 (s) ν_{as}(COO), 1566 (s), 1528 (s) and 1453 (s) ν_s(COO), 1377 (s), 1320 (m), 1253 (s), 1142 (m) and 1066 (s) ν(C−X) (X = C, N, O), 887 (m), 834 (w), 768 (m), 712 (w), 639 (w), 585 (w).

[Cu_4(μ_4-Hetda)$_2$(Hpmal)$_2$(H_2O)]·7.5H_2O (**8**) Anal. calcd for **8**: $Cu_4C_{38}H_{73}N_4O_{24.5}$ (MW 1232.2): C 37.04, H 5.97, N 4.55; found: C 37.03, H 5.50, N 4.54. Compound **8** is slightly soluble in H_2O, MeOH and EtOH. IR (KBr): 3419 (s br) ν(OH), 2856 (m) ν_s(CH), 1624 (s) and 1597 (s) ν_{as}(COO), 1409 (m) ν_s(COO), 1274 (w), 1059 (m) ν(C−X) (X = C, N, O), 906 (w), 730 (m), 637 (w), 504 (w).

Catalytic studies

The cyclohexane oxidation was typically carried out in air atmosphere in round flasks equipped with a condenser, under stirring at 50 °C and using MeCN as solvent (up to 5.0 mL total volume). In a typical experiment, a solid pre-catalyst **5**–**8** was introduced (0.01 mmol) into the reaction mixture,

followed by the addition of an acid co-catalyst (0.1 mmol). Finally, cyclohexane (2 mmol) was introduced and the reaction started after the addition of hydrogen peroxide (50% in H_2O, 10 mmol).

The reactions were monitored by removing small aliquots after different periods of time, which were treated with PPh_3[9]. The samples were analyzed by gas chromatography (GC) using nitromethane as an internal standard. Attribution of peaks was made by comparison with chromatograms of authentic samples. GC analyses were run on an Agilent Technologies 7820A series gas chromatograph (He as carrier gas) equipped with FID detector and BP20/SGE (30 m × 0.22 mm × 0.25 μm) capillary column.

Results and Discussion

Spectroscopic characterization

The IR spectra of **1**–**8** show comparable features due to the presence of copper(II) aminoalcohol blocks, aromatic carboxylate ligands and water molecules. Hence, the characteristic vibrations include one or two $\nu(H_2O)/\nu(OH)$ bands with maxima in the 3510–3185 cm^{-1} range due to H_2O molecules and OH groups of aminoalcohol ligands, the broad character of which is indicative of intensive hydrogen bonding. The ν_{as} and ν_s CH vibrations are observed as two to four typically weak bands in the 3020–2830 cm^{-1} range. Besides, the spectra of **1**–**8** also reveal the two pairs of strong ν_{as}(COO) [1617–1600 and 1585–1560 cm^{-1}] and ν_s(COO) [1395–1385 and 1352–1362 cm^{-1}] bands of the carboxylate linkers. The ESI−MS(+) plots of **1**–**3** show several Cu-aminoalcohol fragments obtained upon removal of nda ligands. Thus, the heaviest $[Cu_2(dmea)_2(H_2O)_2 + 2H_2O - H]^+$ (*m/z* 373), $[Cu_2(Hmdea)_2 - H]^+$ (*m/z* 361) and $[Cu_2(Hbdea)_2 - H]^+$ (*m/z* 445) fragments with the expected isotopic distribution pattern were detected in **1**–**3**, respectively. In these compounds, other characteristic peaks correspond to further fragmentation with the loss of one aminoalcohol moiety and/or one Cu atom. The ESI−MS(+) spectrum of **4** exhibits the characteristic $[Cu_2(Hetda)]^+$ (*m/z* 362) and $[Cu(nda) + H]^+$ (*m/z* 278) peaks. The ESI−MS(–) plots of all compounds are less informative, showing the highly intense peaks due to the $[Hnda + 2H_2O]^-$ (*m/z* 251 in **1** and **4**) or $[Hnda]^-$ (*m/z* 215 in **2** and **3**) fragments.

Thermogravimetric analysis[10,11]

The TGA analyses have been performed under a N_2 atmosphere in the 30–750 ºC range to evaluate the thermal behaviour of **1**–**6**. The compounds **2** and **3** showed similar characteristics within the 80–410 ºC temperature range. The first endothermic effect of **2–4** corresponded to the elimination of crystallization water molecules, namely two for **2** and **3** and 2.5 for **4** and it occurred within the 80–200 ºC temperature range, whereas for compound **1** the elimination of two crystallization H_2O molecules was initiated only at 220 ºC. The decomposition of the aminoalcohol in **1–4** was observed in the 200–340 ºC temperature range. Further thermal effects with maxima at 370 ºC (in **1**), 300°C and 390 ºC (in **2**), 320ºC (in **3**) and 445 ºC (in **4**) are due to the multistep elimination of nda fragments. In **5** the elimination of one crystallization H_2O molecule is observed during the endothermic effect that occurred in the 50–140 ºC temperature range. The removal of the one H_3bis-tris moiety in **5** and two H_2tea moieties in **6** was observed in the 215–270 ºC temperature range. The second H_3bis-tris fragment and two Hhpa ligands in **5** decompose in the 240–450 ºC range whereas in **6** the complete removal of two hpa fragments occurred in the 270–450 ºC temperature range.

Description of crystal structures[10,11]

The crystal structure of the linear 1D coordination polymer **1** is based on a dicopper(II) $[Cu_2(\mu\text{-dmea})_2(H_2O)_2]^{2+}$ block, a μ-nda(2–) linker and two

crystallization H_2O molecules (Figure 3a). Similarly to **1**, the structures of **2** (Figure 3b) and **3** also feature the 1D metal-organic chains assembled from the related $[Cu_2(\mu\text{-Hmdea})_2]^{2+}$ or $[Cu_2(\mu\text{-Hbdea})_2]^{2+}$ blocks and μ-nda linkers. However, in these dicopper(II) blocks the axial site around the Cu atom is not occupied by the H_2O ligand, but by the OH group from an additional CH_2CH_2OH arm of the aminoalcohol moiety.

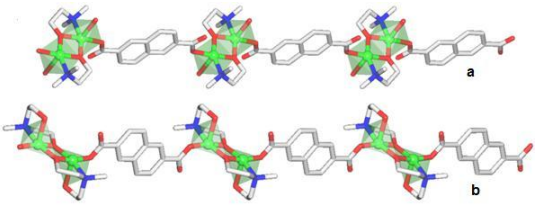

Figure 3. Structural fragments of **1** (a) and **2** (b) showing linear 1D metal-organic chains with polyhedral representation of the coordination environments around Cu atom. H atoms and crystallization H_2O molecules are omitted for clarity. Color codes: Cu balls (green), O (red), N (blue) and C (gray).

Compound **4** reveals a discrete 0D structure composed of dicopper(II) $[Cu_2(H_4etda)_2(\mu\text{-nda})]^{2+}$ cation, nda(2–) anion and four crystallization H_2O molecules (Figure 4).

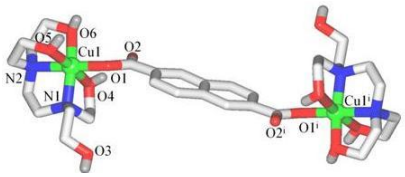

Figure 4. Structural fragments of **4** with atom numbering scheme. H atoms (except those of H_2O or OH moieties), crystallization H_2O molecules and nda^{2-} anion (in **4**) are omitted for clarity. Color codes are those of Figure 3.

The cation bears two symmetric equivalent $\{Cu(H_4etda)\}^{2+}$ blocks that are interconnected by the bridging 2,6-naphthalenedicarboxylate. The discrete 0D structure of **5** consists of the neutral tricopper(II) $[Cu_3(\mu_2\text{-}H_3bis\text{-}tris)_2(\mu_2\text{-Hhpa})_2]$ unit and a half crystallization water molecule. It has a symmetric linear $[Cu_3(\mu\text{-O})_4(\mu\text{-COO})_2]$ core (Figure 5).

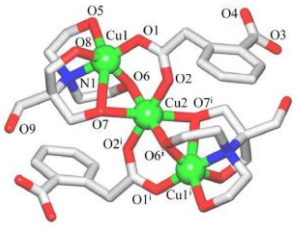

Figure 5. Structure of **5** showing tricopper(II) unit with atom numbering scheme. H atoms and crystallization H_2O molecules are omitted for clarity. Color codes are those of Figure 3.

The crystal structure of **6** discloses a *zigzag* 1D coordination polymer assembled from the repeating tricopper(II) $[Cu_3(\mu_2\text{-}H_2tea)_2(\mu_2\text{-hpa})(\mu_3\text{-hpa})]$ units with an asymmetric $[Cu_3(\mu\text{-O})_3(\mu\text{-COO})_2]$ core (Figure 6).

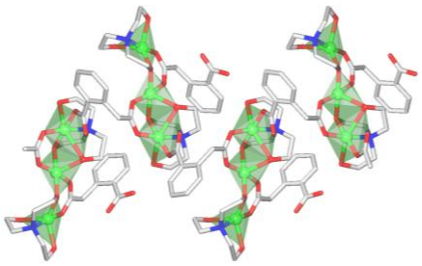

Figure 6. Structural fragments of **6** showing the *zigzag* 1D metal-organic chain with polyhedral representation of the coordination environments around Cu atom. H atoms are omitted for clarity. Color codes are those of Figure 3.

The compound **7** is a 1D coordination polymer, the structure of which is composed of the repeating tetracopper(II) $[Cu_4(H_2etda)_2(sal)_2]$ units (Figure 7a) and ten crystallization water molecules. The adjacent Cu_4 blocks reveal a single-open cubane $[Cu_4(\mu_2\text{-O})(\mu_3\text{-O})_3]$ core and are interconnected via one of the hydroxyethyl arms of the H_2etda ligand, forming an infinite metal-organic chain (Figure 7a,b).

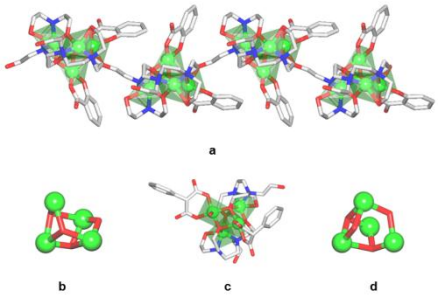

Figure 7. (a) 1D coordination polymer chain of **7** with the coordination polyhedra around the copper atom, (b) distorted single-open cubane $[Cu_4(\mu_2\text{-O})(\mu_3\text{-O})_3]$ core of

7, (c) tetracopper block of compound **8** with coordination polyhedra around the copper atom, (d) distorted double-open cubane $[Cu_4(\mu_2\text{-}O)_2(\mu_3\text{-}O)_2]$ core of **8**.

The discrete 0D structure of **8** bears the neutral tetracopper(II) $[Cu_4(Hetda)_2(Hpmal)_2(H_2O)]$ unit (Figure 7c). Although this Cu_4 unit resembles that of **7**, there are a few differences that consist in: (i) the compound dimensionality (0D in **8** *vs.* 1D in **7**), (ii) the presence of two monoprotonated μ_4-Hetda ligands in **8** *vs.* μ_4- and μ_5-H_2etda in **7** and (iii) the existence of three five-coordinate (Cu1, Cu3, Cu4) and one six-coordinate (Cu2) copper atoms in **8** *vs.* a pair of five- and six-coordinate copper atoms in **7**. These differences lead to the formation of a distinct double-open cubane $[Cu_4(\mu_2\text{-}O)_2(\mu_3\text{-}O)_2]$ core in **8** (Figure 7d).

Topological analysis of H-bonded networks of 1–8[10,11]

An intense pattern of intermolecular (O–H···O) hydrogen bonds provides the extension of the structures into distinct supramolecular networks [1D → 3D (**1**, **2**, **7**), 1D → 2D (**3**, **6**) and 0D →3D (**4**, **5**, **8**)]. The topological analysis was performed after simplification of the supramolecular networks following the concept of underlying net[12], revealing some rare (**1**, **3**, **5**, **6**) or even undocumented (**2**, **4**, **7** and **8**) topological types.

Magnetic properties of 1–6[10,11]

The magnetic properties of **1**–**4** (Figure 8), **5** and **6** (Figure 9) were investigated over the temperature range of 1.8–300 K. For that purpose the magnetic susceptibility $\chi_m T$ *vs.* *T* was studied.

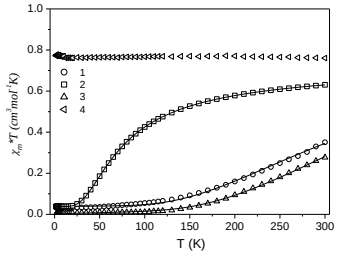

Figure 8. Temperature dependence of experimental $\chi_m T$ (χ_m per 2 Cu^{II} atoms) for **1**–**4**.

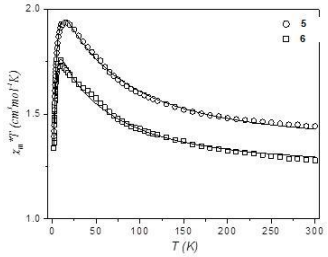

Figure 9. Temperature dependence of experimental $\chi_m T$ (χ_m per 3 Cu^{II} atoms) for **5** and **6**.

The magnetic susceptibility studies of **1**–**3** indicate a strong antiferromagnetic coupling between the Cu(II) atoms through the μ-alkoxo bridges, so the compounds behave as antiferromagnetically coupled dicopper(II) derivatives [J = –470(2), –100(2) and –590(1) cm^{-1}, respectively] whereas **5** and **6** showed a predominant ferromagnetic coupling [J = 39.1(1) and 29.5(1) cm^{-1}, respectively] within the mixed-bridged tricopper(II) cores. However, **4** has no significant magnetic interaction within the dicopper(II) units.

Mild catalytic oxidation of cyclohexane of 5–8

The compounds **5–8** have been applied as pre-catalysts for the mild homogeneous oxidation of cyclohexane by aqueous H_2O_2 in acetonitrile solution and in the presence of an acid promoter (co-catalyst), resulting in the formation of the corresponding alcohol and ketone. It was observed that the C_6H_{12} oxidations catalyzed by the **5–8**/TFA systems (TFA = trifluoroacetic acid) achieve 27% of the maximum total product yield, based on substrate.

We have observed that pre-catalysts **5**–**8** are almost inactive unless a small amount of an acid is added. Aiming at verifying whether the type of acid (co-catalyst) has an influence on the efficiency of the catalytic system, we have tested different acids (TFA, HCl, H_2SO_4 and HNO_3) in the oxidation of C_6H_{12} with **5** (Figure 11a[11]), **7** (Figure 11b) and **8** (Figure 11c) as pre-catalysts. Despite the addition of TFA or H_2SO_4 leads to the maximum total product yields, the oxidation is exceptionally quick

in the presence of HCl. The oxidation of C_6H_{12} also proceeds with HNO_3 as co-catalyst despite being slower than in the system with TFA.

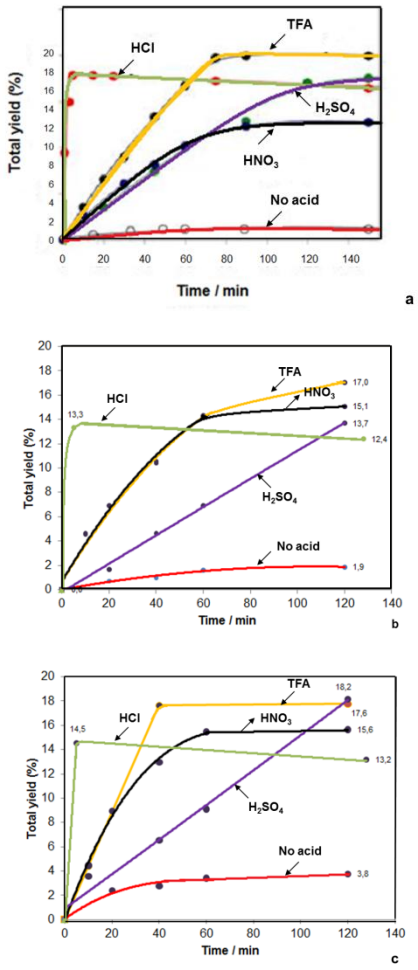

Figure 11. Oxidation of cyclohexane to cyclohexanol and cyclohexanone by H_2O_2 catalysed by (a) **5**[11], (b) **7** and (c) **8**. Evolution of the total product yield with time in the absence and in the presence of different acid co-catalysts (HNO_3, H_2SO_4, HCl, TFA; 0.1 mmol).

Although addition of TFA provided the maximum total products yield of 20% for **5**–**8**, the oxidation is exceptionally quick in the presence of HCl resulting in a comparable maximum total yield of 18% for **5** achieved in only 5 min reaction time[11]. The oxidation of C_6H_{12} also proceeds with H_2SO_4 as a co-catalyst providing a maximum total yield of 18% for **5** and **8**. Surprisingly, H_2SO_4 was the most efficient co-catalyst for **8** (Figure 11c). In contrast, HNO_3 showed a weaker promoting behavior with maximum total yield of 12–16% for **5**, **6** and **8**. However, for **7** HNO_3 showed a similar promoting behavior as TFA until 60 min reaction time. Furthermore, we have studied the effect of TFA amount on the total product yield. Different optimum TFA amounts were observed for each pre-catalyst. Thus, the maximum total products yield corresponded to the molar ratio of 1:10 in **5**[11], 1:2 in **7** and 1:5 in **8**. The maximum yield achieved (27%) was in the system in which we used TFA as co-catalyst. Such an observation suggests that TFA is necessary to activate the pre-catalyst, presumably via additional protonation and partial decoordination of aminoalcohol and carboxylate moieties.[13]

Conclusions

Herein we described the self-assembly synthesis of new complexes and/or coordination polymers. They were characterized by IR spectroscopy, ESI(±)MS, TGA, elemental and single crystal X-ray diffraction analyses. It was found that compounds **1**–**3** are 1D coordination polymers assembled from dicopper(II) aminoalcohol blocks and μ-nda linkers, **4** is a discrete 0D dimer composed of two $[Cu(H_4etda)]^{2+}$ fragments interlinked by the μ-nda moiety, **5** is a discrete 0D trimer with symmetric $[Cu_3(\mu\text{-}O)_4(\mu\text{-}COO)_2]$ core, **6** is a *zigzag* 1D coordination polymer with asymmetric $[Cu_3(\mu\text{-}O)_3(\mu\text{-}COO)_2]$ core, **7** is a 1D coordination polymer, with a single-open cubane $[Cu_4(\mu_2\text{-}O)(\mu_3\text{-}O)_3]$ core and **8** is a 0D tetramer with a double-open cubane $[Cu_4(\mu_2\text{-}O)_2(\mu_3\text{-}O)_2]$ core.

An intense pattern of intermolecular (O–H···O) hydrogen bonds provided the extension of the structures into distinct supramolecular networks [1D → 3D (**1**, **2**, **7**), 1D → 2D (**3**, **6**) and 0D →3D (**4**, **5**, **8**)] which were topologically analysed. The magnetic susceptibility studies revealed a strong antiferromagnetic coupling between the Cu(II) atoms through the μ-alkoxo bridges in **1**–**3** and a predominant ferromagnetic coupling within the

mixed-bridged tricopper(II) cores in **5** and **6**. Finally, it was confirmed that compounds **5**–**8** can act as rather efficient bio-inspired pre-catalysts for the mild homogeneous oxidation of cyclohexane to the corresponding alcohol and ketone, by aqueous H_2O_2 at 50°C in acidic MeCN/H_2O medium, with overall yields up to 27% based on the alkane.

This work was important to: (i) extend the diversity of copper(II) coordination polymers and multinuclear complexes assembled from aminoalcohols and aromatic carboxylate ligands, (ii) give new insights on the topological studies, resulting on the discovery of unreported topological types, (iii) study their magnetic properties and (iv) evaluate their catalytic efficiency for the mild oxidation of cyclohexane. Further research on broadening the types of self-assembled copper(II) coordination polymers and multinuclear complexes derived from various aminoalcohols and search for their applications in molecular magnetism and in oxidation catalysis is underway.

Acknowledgments

This work was supported by the FCT (projects PTDC/QUI-QUI/121526/2010, RECI/QEQ-QIN/0189/2012, PEst-OE/QUI/UI0100/2013, IF/01395/2013 and SFRH/BPD/78854/2011), Portugal.

References

1. C. Santini, M. Pellei, V. Gandin, M. Porchia, F. Tisato, C. Marzano, *Chem. Rev.*, 2014, **114**, 815.

2. S. R. Batten, D. R. Turner, S. M. Neville, *Coordination Polymers: Design, Analysis and Application*, Royal Society of Chemistry: London, 2009.

3. A. M. Kirillov, M. V. Kirillova, A. J. L. Pombeiro, *Coord. Chem. Rev.*, 2012, **256**, 2741.

4. (a) H. Eagle, *Science*, 1971, **174**, 500; (*b*) K. H. Scheller, T. H. Abel, P. E. Polanyi, P. K. Wenk, B. E. Fischer, H. Sigel, *Eur. J. Biochem.*, 1980, **107**, 455; (*c*) R. Beynon, J. Easterby, *Buffer Solutions Basics*, Oxford Univ. Press Inc., New York, 1st edn, 1996.

5. See the Cambridge Structural Database (CSD, version 5.35, 2014) F. H. Allen, *Acta Crystallogr., Sect. B*, 2002, **58**, 380.

6. A. M. Kirillov, Y. Y. Karabach, M. Haukka, M. F. C. Guedes da Silva, J. Sanchiz, M. N. Kopylovich, A. J. L. Pombeiro, *Inorg. Chem.* 2008, **47**, 162.

7. A. M. Kirillov, Y. Y. Karabach, M. V. Kirillova, M. Haukka, A. J. L. Pombeiro *Cryst. Growth Des.* 2012, **12**, 1069.

8. A. M. Kirillov, M. N. Kopylovich, M. V. Kirillova, M. Haukka, M. F. C. G. da Silva, A. J. L. Pombeiro, *Angew. Chem. Int.* 2005, **44**, 4345.

9. G. B. Shul'pin, *J. Mol. Catal. A: Chem.*, 2002, **189**, 39.

10. S. S. P. Dias, V. Andre, J. Klak, M. T. Duarte, A. M. Kirillov *Cryst. Growth Des.* 2014, **14**, 3398.

11. S. S. P. Dias, M.V. Kirillova, V. Andre, J. Klak, A. M. Kirillov *Inorg. Chem. Frontiers*. 2014 (submitted).

12. (a) V. A. Blatov, A. P. Shevchenko and D. M. Proserpio, *Cryst. Growth Des.*, 2014, **14**, 3576; (*b*) V. A. Blatov, *IUCr CompComm Newsletter*, 2006, **7**, 4.

13. A. M. Kirillov, M. V. Kirillova, L. S. Shul'pina, P. J. Figiel, K. R. Gruenwald, M. F. C. G. da Silva, M. Haukka, A. J. L. Pombeiro, G. B. Shul'pin, *J. Mol. Catal. A: Chem.*, 2011, **350**, 26.